Effect of Shroud Hole on the Force Characteristics of a Circular Cylinder

M.F. Osrin, A.M. Azmi, H.Yusoff, N.A. Razak

Abstract: ***Characteristics of flow pass a shrouded cylinder were investigated experimentally using uniform and non-uniform hole shrouds. The experiments were performed to compare the effect of hole-uniformity of the perforated shroud on the cylinder lift and drag. The porosity for uniform hole shrouds in triangular and square configurations were set around 0.30, while that for non-uniform hole shrouds were set from 0.25 to 0.37. The diameter ratio between the shroud and the bare cylinder was set at 2.0. The experiment was performed in a wind tunnel at Reynolds Number of 9.345 x 10^3 based on the bare cylinder diameter and constant incoming air flow speed. Results showed that although all shrouded cylinder models reduced drag significantly in comparison to that of the bare cylinder case, the non-uniform hole shrouds were considerably effective than the uniform hole shrouds. Total drag reduction achieved by the non-uniform hole shrouds of 30% porosity was between 90-95% whereas that of uniform hole was only 55-80% at the same porosity.***

Keywords **: non-uniform hole, perforated shroud, vortex suppression, vortex shedding**

I. INTRODUCTION

Fluid flow over a bluff body is commonly found in nature and engineering application. The external fluid flow that interacts with the bluff body normally produce unsteady flow characteristic and high amplitude of fluctuating force which contribute to vortex induced vibration (VIV). The flow over bluff body such as cylinder has been a subject of many studies for researchers due to its application in a chimney, oil rigs, pipelines, piers, bridge cable, buildings and tower. These structures may experience structural failure during their lifespan due to Vortex-Induced Vibration. The general review on VIV is mostly on the cylindrical body [1]–[3]. For the past decade, many attentions have been given to attenuate the effect of VIV on cylinder due to industrial demand. In order to reduce or eliminate VIV, it is essential to alter the mechanical properties of the material used or control the flow structure around the body. Every et al. [4] review that flow can be controlled with suppression devices that alter the structural profile and prevent the vortex shedding along the length of the structures.

The passive devices using streamlining principle like fairings and splitter plates have great demand in industries [5]–[7], however, they are only unidirectional to the flow. Some of the devices are flexible, but this passive device depends on maintenance and their ability to align with the flow [7]–[9]. Lou et. al. [10] investigate the fairing model at angles of 45°, 60°, 75° and 90°. The effect of VIV shows effective reduction at caudal horn angles of 45° and 60° of the configuration. The drag load for upstream riser can be reduced with the position of two risers in a tandem arrangement, but for downstream riser the drag load will increase. The result of the drag load can be reduced for both upstream and downstream with the configuration of risers arranged side-by-side.

Other passive devices that have been studied in the past are shrouds. The examples of shrouds are control rods [11]–[13], wire mesh[14]–[16], flexible mesh [17] and perforated shrouds [18]–[20]. The Perforated shrouds have been extensively used in several studies placed in shallow water [21], [22] and deep water [15], [18], [19], [23], [24] with the purpose of suppressing VIV. Gozmen and Akilli [15] studied the flow around bare cylinder case, shrouded with a permeable cylinder at Reynolds number of 5000 in deep water. The permeable cylinder was of 0.4 to 0.85 porosities. It was found that gap ratio of 3.0 at the porosity range of 0.5 to 0.7, was the most effective where the effect of the permeable cylinder increase tremendously, and the turbulent statics decreased by 70% for 70% porosity.

In comparison to strakes, fairings and other passive devices, shrouds have the advantages of suppressing vibration without increasing the drag and they are omnidirectional. However, research on shrouds were not exhaustive, and they are limited to only uniform hole; no existing studies were carried out on non-uniform hole. It is believed that non-uniform hole shroud would further prevents vortex shedding becoming correlated along the span, reducing the correlation, enhancing three-dimensionality of the flow, thus decreasing the drag. The present research aims to examine the effect of different hole-configurations of the shrouds on the force characteristics of the bare cylinder. The results are then compared to that of a plain circular cylinder. The shroud hole-arrangements are tested in square and triangular pattern at low porosity.

Revised Manuscript Received on 20 October, 2019.
***** Correspondence Author
M.F. Osrin, Faculty of Mechanical Engineering, Universiti Teknologi MARA, Shah Alam, Selangor, Malaysia, mohamadfaizbinosrin@gmail.com
A.M. Azmi*, Faculty of Mechanical Engineering, Universiti Teknologi MARA, ShahAlam, Selangor, Malaysia, azlinazmi@salam.uitm.edu.my
H. Yusoff, Faculty of Mechanical Engineering, Universiti Teknologi MARA, Cawangan Pulau Pinang, Permatang Pauh, Pulau Pinang, Malaysia, hamidyusoff@uitm.edu.my
N.A. Razak, School of Aerospace Engineering, Universiti Sains Malaysia, Engineering Campus, 14300 Nibong Tebal, Pulau Pinang, norizham@usm.my

II. METHODOLOGY

A. Cylindrical Test Model

The bare cylinder and perforated shrouds used in this study were fabricated using 3D printing made of polylactic acid (PLA) material. The bare cylinder diameter, d is 12.7mm and perforated shrouds diameter, D is 25.4mm, respectively and spanwise length of 300mm. The thickness of the shrouds was 2 mm. The porosity, β is defined as the ratio between the open area of the cylinder to the total area of the cylinder. These shrouds have different hole-arrangements, arranged in square and triangular configurations. For uniform holes, the radius was set as r, while for non-uniform holes, the radius was set at 0.5r, r, and 2r for triangular pattern and 0.5r, r, 2r and 3r for square pattern as shown in Fig.1 and calculated using equation (1). The choice of r was based on the consistency of the low porosity values (within the range of 0.25 to 0.37) for fair comparisons between different shrouds at low porosity. A shroud of random holes was generated for further insight on the force characteristic. The effect of hole-configurations was examined using seven different shrouds, as shown in Table I. Fig.2 and Fig.3 show the uniform and non-uniform hole configurations and diagrams of cut away view of the perforated shrouds.

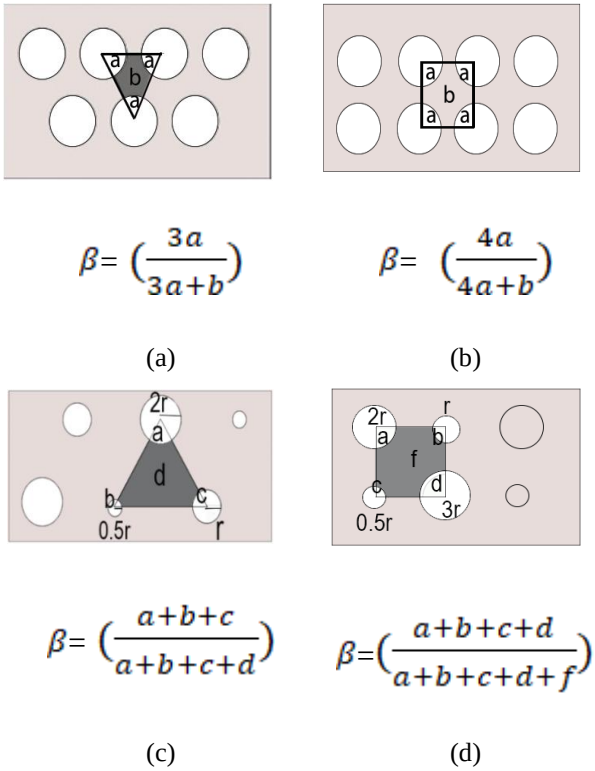

$$\beta = \left(\frac{3a}{3a+b}\right) \qquad \beta = \left(\frac{4a}{4a+b}\right)$$

$$\beta = \left(\frac{a+b+c}{a+b+c+d}\right) \qquad \beta = \left(\frac{a+b+c+d}{a+b+c+d+f}\right) \quad (1)$$

Fig. 1. Hole-configurations and porosity definition; a) uniform-hole triangular pattern, b) uniform-hole square pattern; c) non- uniform hole triangular pattern, d) non-uniform hole square pattern

Table I: Properties of perforated shroud

Perforated Shroud	Porosity (β)	Uniformity
Uniform square pattern (US31)	0.31	Uniform
Uniform triangular pattern (UT30)	0.30	Uniform
Non-uniform square pattern (NuS37)	0.37	Nonuniform
Non-uniform triangular pattern (NuT25)	0.25	Nonuniform
Non-uniform random pattern (R)	Not measured	Nonuniform
Non-uniform square pattern (NuS30)	0.30	Nonuniform
Non-uniform triangular pattern (NuT30)	0.30	Nonuniform

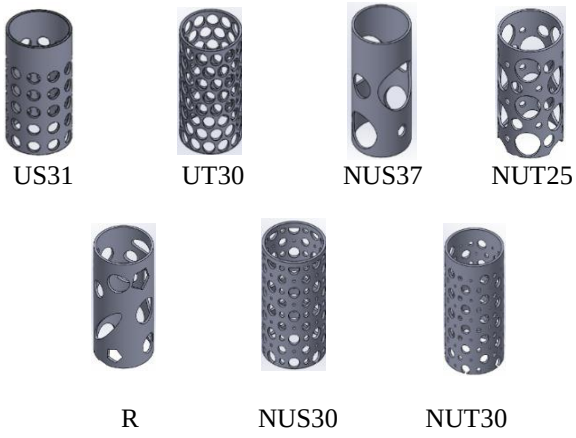

Fig. 2. Perforated shrouds model

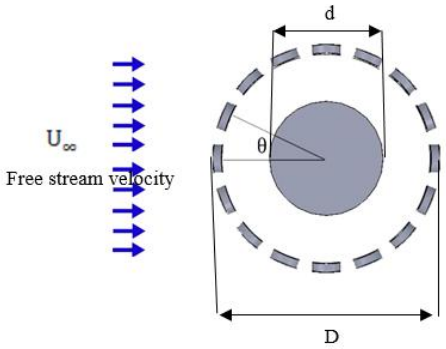

Fig. 3. Schematic drawing cutaway view of perforated shroud

B. Experimental Setup

The test models were placed in a wind tunnel setup at School of Aerospace Engineering, Universiti Sains Malaysia. The test section of open circuit wind tunnel was 320mm wide x 350mm high x 300 mm long, with transparent wall. The cylinder model was mounted horizontally inside the wind tunnel and attached to a balancing force to measure the lift and drag forces. The blockage ratio based on the bare cylinder model was 3.6%. The cylinder models was tested in an open channel subsonic wind tunnel setup as shown in Fig.4. For lift and drag measurement, this bare cylinder case was mounted horizontally in the wind tunnel and attached to a connection of balancing force placed outside the wind tunnel. The connection of balancing force was used to detect the lift and drag forces in term of voltage. The input from the balancing force was transferred to the data acquisition device (Kyowa PCD 300A) that connected to a computer. The data was analyzed using PCD300A software. The lift and drag data was recorded for 10 seconds.

For pressure measurement, the bare cylinder model was set up horizontally in wind tunnel similar to lift and drag experiment. The pressure distribution around the bare cylinder model was measured by using pressure sensor (MPXV 7002). The pressure tap was created on the bare cylinder surface at the center position and rotated for every 10^o on the pressure measurement plane. The data acquisition time was set up for 10 seconds.

The pressure tap was connected to a polyvinyl tube (PVC) with 0.55m in length and 0.9mm inner diameter. The pressure voltage taken was converted to pressure coefficient, C_p by using the equation (2) where p is the static pressure on cylinder model, U_∞ is the incoming flow, and p_∞ is the static pressure of the incoming airflow

$$C_p=\frac{p-p_\infty}{\frac{1}{2}p_\infty U_\infty{}^2}, \qquad (2)$$

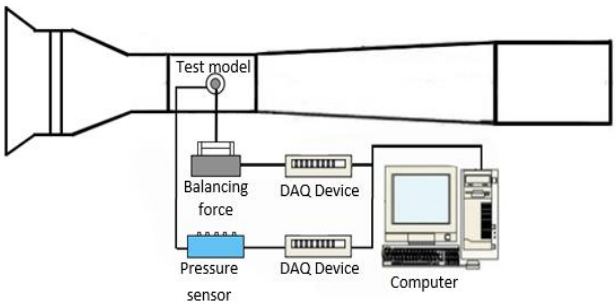

Fig. 4. Schematic diagram for lift drag at wind tunnel setup

III. RESULTS

A. Pressure Coefficient

Fig.5(a) shows the distribution of mean pressure coefficient on the surface of the cylinder model for baseline case and perforated shrouded cylinder cases. The result of the bare cylinder for subcritical region is validated by the bare cylinder results of L. Feng and J. Wang, as well as M. M. Zdravkovich and J. R. Volk [25],[26]. For baseline case at $\theta \approx 0^o$-70^o section, the surface pressure is recovered gradually on the windward face of the cylinder starting from C_p=1 to C_p=-1.4. At $\theta \approx 70^o$-90^o, the surface pressure undergo recovery and developed a negative pressure gradients on the test model. The leeward side of the test model presents a result of plateau region with constant low pressure along $\theta \approx 90^o$-270^o. The pressure difference between a windward and a leeward section of cylinder result in drag force effect on the cylinder model. The decrease of pressure difference will lead to the reduction of drag force by means of lifting of plateau region at the leeward section of the cylinder.

The pressure distribution of perforated shrouds shows similar behaviour to findings of Gao et al. [27], Chen et al.[28], and Gu et al. [8] who used similar perforation mechanism. All perforated shrouds cases show pressure lines are lifted substantially above the baseline cylinder case at the leeward section, indicative of drag suppression. The NuS30 and NuT30 cases show C_p falls below 1 at $\theta = 0^o$. This is due to the solid blockage of perforated shrouds that blocked the pressure tap horizontally to the incoming flow.

Fig.5(b) shows the root mean square (RMS) values of the instantaneous pressure coefficient or the fluctuating pressure distribution, C_p' around a circular cylinder. The result of C_p' is obtained by applying RMS of C_p data. This C_p' represents the unsteadiness of wind load acting on the cylinder. The C_p' result at the leeward section of cylinder with perforated shrouds are smaller compared to baseline case. It agrees with the result of Gao et al., Chen et al., and Gu et al. as controlled cases have lower C_p' compared to baseline [27],[28],[8]. Thus, from Fig.5 show that the results of perforated shrouds cylinder significantly contribute to lower the drag and suppress the unsteady dynamic wind load.

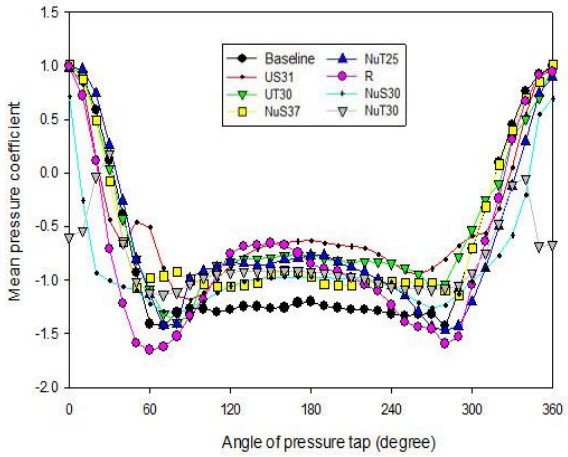

(a)

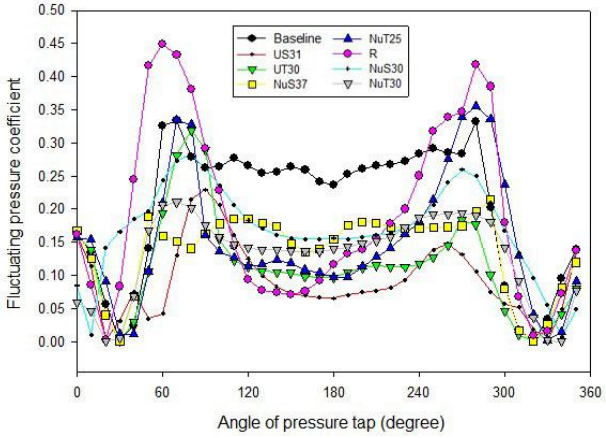

(b)

Fig. 5. Pressure distribution; (a) Mean pressure distributions, (b) Fluctuating pressure distributions

B. Lift Coefficient

Fig.6 show time histories of lift coefficients, C_l of baseline case and perforated shroud cases. The black line denoted the baseline case, while the red lines represent the perforated shroud cases of different configurations. The behaviour of C_l for perforated shrouds are different in amplitudes from that observed in baseline case. The presence of shrouds control the wake structure and entrainment layer behind bare cylinder. Thus, the cylinder is exempted from vortex induced vibration. For the baseline case, the graph of C_l shows highly unsteady amplitudes fluctuation. This is due to the unsteady vortex shedding in the near wake of the cylinder. As shown in Fig.6, all the controlled cases with perforated shrouds cylinder significantly damped the fluctuation amplitudes of the instantaneous lift force.

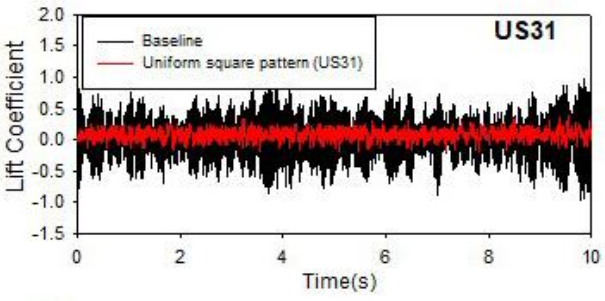

(a)

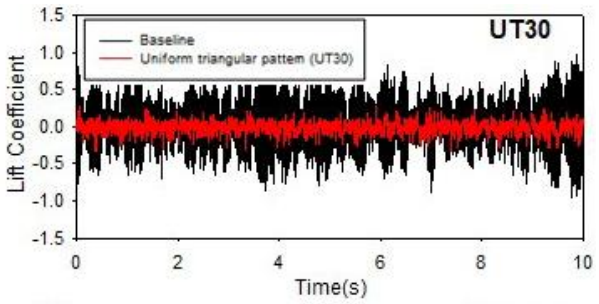

(b)

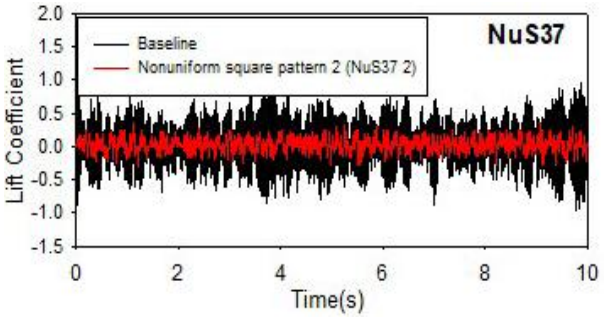

(c)

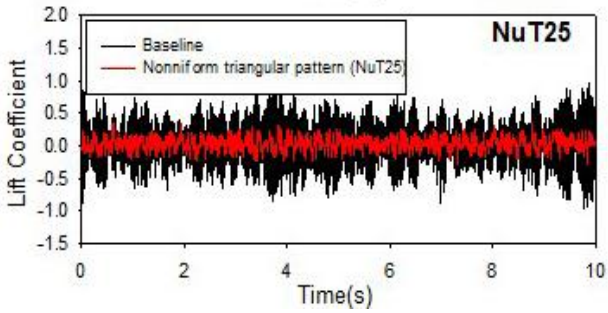

(d)

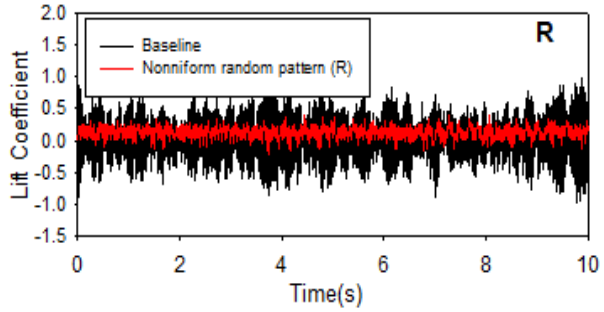

(e)

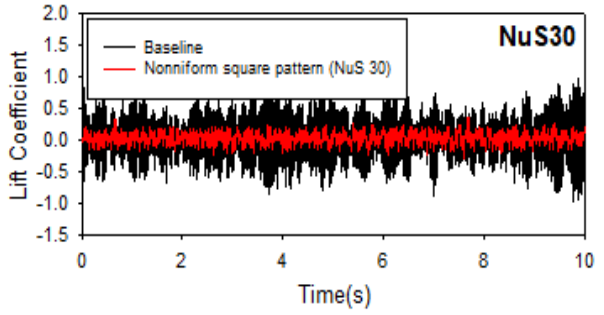

(f)

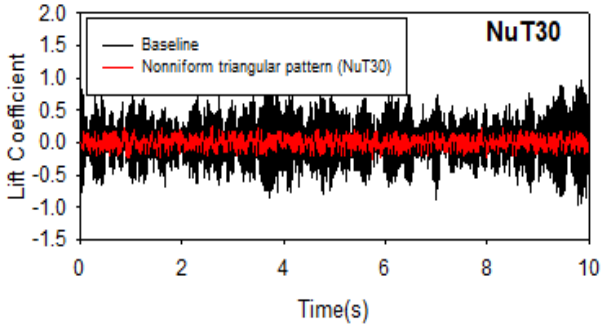

(g)

Fig. 6. Time histories of lift coefficient for, uniform and nonuniform holes perforated shroud cases of, (a) US31, (b) UT31, (c) NuS37, (d) NuT25, (e) R, (f) NuS30, (g) NuT30

C. Drag Coefficient

Fig.7 shows the time histories of mean drag coefficients, C_d for baseline case and perforated shroud cases. The unsteady amplitude of C_d for baseline case is at the average of C_d=1.0, while the C_d of perforated shrouds cases fall below the baseline case. The value of the mean drag is also tabulated in **Table II.** This reveal that the C_d can be effectively reduced by applying perforated shrouds cylinder. The mean drag coefficient for US31 and UT30 are reduced to 0.2 and 0.45 which give reduction of 80% and 55% in comparison to that of the baseline case. The R, NuS30 and NuT30 cases give the best drag reduction of around 90-95%, in comparison to other cases and much larger reduction than that of baseline case. In addition, for non-uniform shroud of porosity below and above 30% of triangle and square configurations, the drag suppression is just 55% and 70%, respectively, not as significant as that of 30% porosity. Further test at other porosity values would conform on the optimum effective porosity for both configurations.

Table II

Mean C_d of cylinder cases and percentage reduction to bare cylinder

Cylinder Cases	Mean C_d	Percentage reduction (%)
Bare cylinder	1.0	-
US31	0.20	80
UT30	0.45	55
NuS37	0.30	70
NuT25	0.45	55
R	0.05	95
NuS30	0.10	90
NuT30	0.05	95

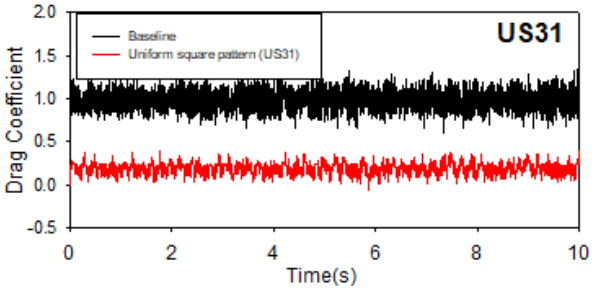

(a)

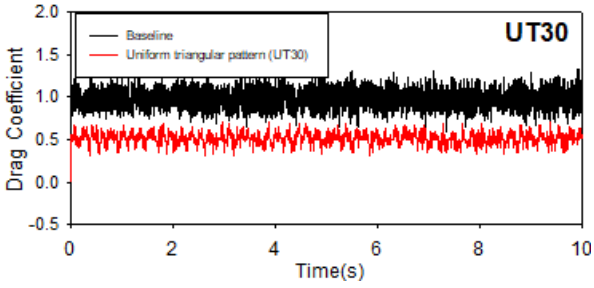

(b)

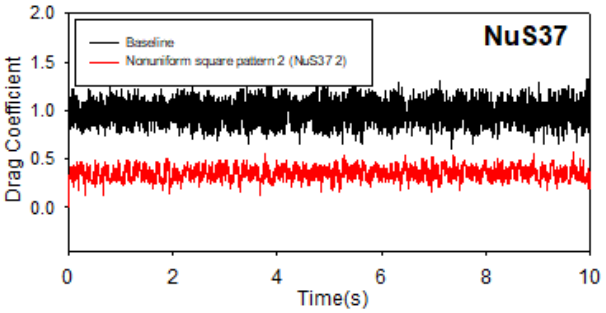

(c)

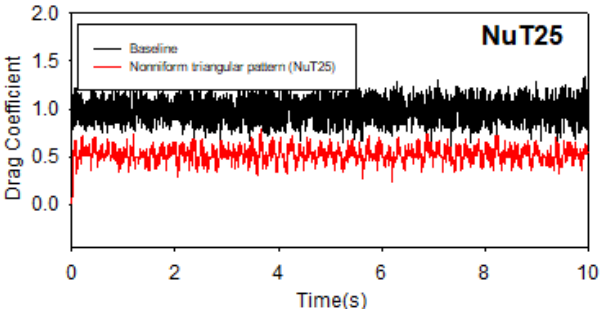

(d)

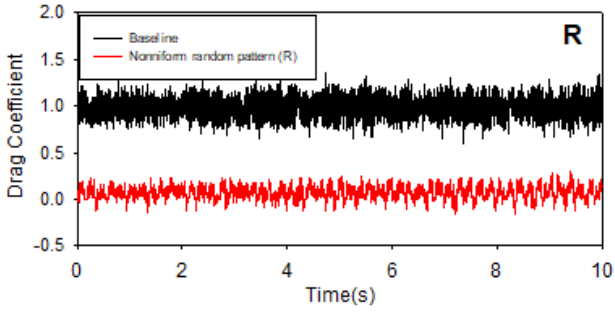

(e)

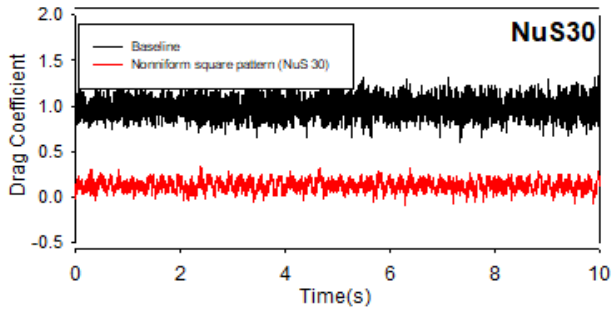

(f)

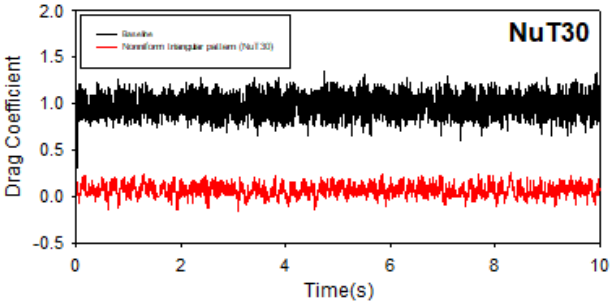

(g)

Fig. 7. Time histories of drag coefficient for, uniform and nonuniform holes perforated shroud cases of, (a) US31, (b) UT31, (c) NuS37, (d) NuT25, (e) R, (f) NuS30, (g) NuT30

IV. CONCLUSION

In this study, flow around a circular cylinder attached with shrouds was studied to investigate the effect of shroud hole on the force characteristics. The shrouds were of uniform and non-uniform holes and the flow was at Reynolds number, Re of 9.345 x 10^3. The presence of the perforated shrouds minimize considerably the fluctuation of lift and reduce the lift coefficient significantly. The non-uniform hole perforated shroud cases (R NuT30 and NuS30) show better drag reduction relative to other cases, suppressing drag by about 90 to 95%. In the future, a spanwise measurement should be conducted to corroborate the vortex correlation and three dimensionality effect discussed earlier.

ACKNOWLEDGMENT

This research was funded by a grant from Ministry of Higher Education of Malaysia (FRGS Grant 600-RMI/FRGS 5/3 (0100/2016)).

REFERENCES

1. M. A.Tognarelli, S. Taggart, and M. Campbell, “Actual VIV fatigue response of full scale drilling risers: with and without suppression devices,” *ASME 27th Int. Conf. Offshore Mech. Arct. Eng.*, vol. 5, pp. 513–525, 2008.
2. C. H. K. Williamson and R. Govardhan, “Vortex-induced vibrations,” *Annu. Rev. Fluid Mech.*, vol. 36, pp. 413–455, 2004.
3. P. W. Bearman, “Vortex shedding from oscillating bluff bodies,” *Annu. Rev. Fluid Mech.*, pp. 195–222, 1984.
4. M.J.Every, R.King, and D.S.Weaver, “Vortex-excited vibrations of cylinders and cables and their suppression,” *Ocean Eng.*, vol. 9, no. 2, pp. 135–157, 1982.
5. G. R. S. Assi, P. W. Bearman, and N. Kitney, “Low drag solutions for suppressing vortex-induced vibration of circular cylinders,” *J. Fluids Struct.*, vol. 25, no. 4, pp. 666–675, 2009.
6. F. J. Huare-Huarte, “On splitter plate coverage for suppression of vortex-induced vibrations of flexible cylinders,” *Phys. Procedia*, vol. 48, pp. 244–249, 2014.
7. G. R. S. Assi, P. W. Bearman, and M. A. Tognarelli, “On the stability of a free-to-rotate short-tail fairing and a splitter plate as suppressors of vortex-induced vibration,” *Ocean Eng.*, vol. 92, pp. 234–244, 2014.
8. F. Gu, J. S. Wang, X. Q. Qiao, and Z. Huang, “Pressure distribution, fluctuating forces and vortex shedding behavior of circular cylinder with rotatable splitter plates,” *J. Fluids Struct.*, vol. 28, pp. 263–278, 2012.
9. S. Teksin and S. Yayla, “Effects of flexible plate attached to the rear of the cylinder on flow structure,” *J. Mech. Sci. Technol.*, vol. 31, no. 3, pp. 1195–1201, 2017.
10. M. Lou, W. gang Wu, and P. Chen, “Experimental study on vortex induced vibration of risers with fairing considering wake interference,” *Int. J. Nav. Archit. Ocean Eng.*, vol. 9, no. 2, pp. 127–134, 2017.
11. H. Wu, D. P. Sun, L. Lu, B. Teng, G. Q. Tang, and J. N. Song, “Experimental investigation on the suppression of vortex-induced vibration of long flexible riser by multiple control rods,” *J. Fluids Struct.*, vol. 30, no. 2, pp. 115–132, 2012.
12. I. Korkischko and J. R. Meneghini, “Suppression of vortex-induced vibration using moving surface boundary-layer control,” *J. Fluids Struct.*, vol. 34, pp. 259–270, 2012.
13. J. I. Jiménez-gonzález and F. J. Huera-huarte, “Vortex-induced vibrations of a circular cylinder with a pair of control rods of varying size,” *J. Sound Vib.*, vol. 431, pp. 163–176, 2018.
14. A M Azmi and T. Zhou, “Passive Control of Vortex Shedding via Screen Shroud,” *Int. Conf. Adv. Technol. Des. Mech. Aeronaut. Eng.*, vol. 234, 2017.
15. B. Gozmen and H. Akilli, “Flow control downstream of a circular cylinder by a permeable cylinder in deep water,” *Wind Struct. An Int. J.*, vol. 19, no. 4, pp. 389–404, 2014.
16. F. J. Huera-Huarte, “Suppression of vortex-induced vibration in low mass-damping circular cylinders using wire meshes,” *Mar. Struct.*, vol. 55, pp. 200–213, 2017.
17. M. M. Cicolin and G. R. S. Assi, “Experiments with flexible shrouds to reduce the vortex-induced vibration of a cylinder with low mass and damping,” *Appl. Ocean Res.*, vol. 65, pp. 290–301, 2017.
18. G. M. Ozkan, T. Durhasan, E. Pinar, M. M. Aksoy, H. Akilli, and B. Sahin, “Vortex shedding control of circular cylinder by perforated shroud in deep water,” *EPJ Web Conf.*, vol. 143, 2017.
19. G. M. Ozkan, T. Durhasan, E. Pinar, A. Yenicun, H. Akilli, and B. Sahin, “Control of the flow in the annular region of a shrouded cylinder with splitter plate,” *EPJ Web Conf.*, vol. 143, 2017.
20. B. Molin, “A potential flow model for the drag of shrouded cylinders,” *J. Fluids Struct.*, vol. 7, no. 1, pp. 29–38, 1993.
21. E. Pinar, T. Durhasan, G. M. Ozkan, M. M. Aksoy, H. Akilli, and B. Sahin, “The effects of perforated cylinders on the vortex shedding on the suppression of a circular cylinder,” *EPJ Web Conf.*, vol. 143, 2017.
22. E. Pinar, G. M. Ozkan, T. Durhasan, M. M. Aksoy, H. Akilli, and B. Sahin, “Flow structure around perforated cylinders in shallow water,” *J. Fluids Struct.*, vol. 55, pp. 52–63, 2015.
23. B. Gozmen, E. Fırat, H. Akilli, and B. Sahin, “Flow control behind a circular cylinder via a porous cylinder in deep water,” *EPJ Web Conf.*, vol. 45, 2013.
24. B. Gözmen, H. Akilli, and B. ŞahiN, “Vortex control of cylinder wake by permeable cylinder,” *Çukurova Univ. J. Fac. Eng. Archit.*, vol. 28, no. 282, pp. 77–85, 2013.
25. L. Feng and J. Wang, “European Journal of Mechanics B / Fluids Modification of a circular cylinder wake with synthetic jet : Vortex shedding modes and mechanism,” *Eur. J. Mech. B/Fluids*, vol. 43, pp. 14–32, 2014.
26. M. M. Zdravkovich and J. R. Volk, “Effect of shroud geometry on the pressure distributed around a circular cylinder,” *J. Sound Vib.*, vol. 20, no. 4, pp. 451–455, 1972.
27. D. L. Gao, W. L. Chen, H. Li, and H. Hu, “Flow around a circular cylinder with slit,” *Exp. Therm. Fluid Sci.*, vol. 82, pp. 287–301, 2017.
28. W.-L. Chen, D.-L. Gao, W.-Y. Yuan, H. Li, and H. Hu, “Passive jet control of flow around a circular cylinder,” *Exp. Fluids*, vol. 56, no. 11, pp. 201, 2015.

AUTHORS PROFILE

Mohamad Faiz Osrin is currently studying Master's Degree(M.Sc) in Mechanical Engineering at Faculty of Mechanical Engineering, Universiti Teknologi MARA. He received his Bachelor Degree at University Sains Malaysia in 2016. He is a registered graduate engineer in Board of Engineers Malaysia (BEM). His main research interest is on fluid flow over bluff body.

Azlin Mohd Azmi is currently serving as Senior Lecturer at the Faculty of Mechanical Engineering, Universiti Teknologi MARA, Shah Alam. She received her Bachelor Degree in Mechanical Engineering from Universiti Teknologi MARA and M.Eng from University of Adelaide. She obtained her Ph.D from University of Western Australia in 2016. She is an associate member of the Energy Institute, U.K and is a Certified Carbon Reduction Manager (CRM). Her research interests include flow-induced vibration suppression and enhancement as well as energy and carbon footprint.

Hamid Yusoff, is currently serving as Senior Lecturer at the Faculty of Mechanical Engineering, Universiti Teknologi MARA, Permatang Pauh. He received his Bachelor Degree in Aerospace Engineering from Universiti Sains Malaysia. He obtained his Ph.D and M.Sc in Mechanical Engineering from Universiti Sains Malaysia. His research interest is in aircraft design, aerodynamics and micro air vehicles.

Norizham Abdul Razak, is currently serving as lecturer at School of Aerospace Engineering, Universiti Sains Malaysia. He received his Ph.D, in Aerospace Engineering, from University of Liege, Belgium in 2012. He obtained his Bachelor Degree and M.Sc in Aerospace Engineering from Uiversiti Sains Malaysia. His interest includes flapping flight, unsteady aerodynamics and aeroelasticity.